DOI: 10.23968/2500-0055-2024-9-1-29-43

OPTIMIZATION OF THE BUILDING-INTEGRATED TRANSPARENT PHOTOVOLTAIC CONFIGURATION BASED ON DAYLIGHT AND ENERGY PERFORMANCE IN SCHOOL BUILDINGS IN THE TROPICS

Susan Susan[1,2]*, Safial Aqbar bin Zakaria[1], Sharifah Fairuz Syed Mohd Fadzil[1]

[1] Universiti Sains Malaysia, Penang, Malaysia
[2] Universitas Ciputra Surabaya, Surabaya, East Java, Indonesia

*Corresponding author's e-mail: susan@student.usm.my / susan@ciputra.ac.id

Abstract

Introduction: Numerous previous studies addressed the use of vertical facades for side lighting. They were found to be an effective daylighting aperture that helps to establish a pleasant environment, improve academic performance in schools, and promote better health. Recent studies also identified the potential for using vertical facades on high-rise buildings as building-integrated photovoltaic (BIPV) systems thanks to the large available area. In the tropics, this potential use is also supported by the availability of abundant solar energy. The technology of transparent PV (TPV) offers the opportunity to meet both needs. It serves as a side lighting aperture and building-integrated transparent photovoltaic (BITPV) depending on several factors, such as the visible transmittance (VT) value and the number of cells. For side lighting, a higher VT value is required to allow for optimal daylight penetration. However, more cell numbers and lower VT are preferable for BITPV. Previous studies found that BITPV is suggested for buildings with a window-to-wall ratio (WWR) of 45 % or more, which seems too high for tropical buildings where the suggested WWR is typically in the range of 30–40 %. **Purpose of the study:** This study aims to find the optimum configuration and present a systematic method for optimizing BITPV for tropical school building facades. **Methods:** An experimental approach using simulation as a tool was employed to achieve the objective. A site with a typical school layout in the tropics was selected as the research context. Treatment based on VT and cell numbers was applied to create several post-test models. **Results and discussion:** In the tropics, when using low-transparency TPV, BITPV with 31.25 % WWR and 30 % cell coverage ratio is found to provide the optimum visual health and comfort, as well as energy performance. Meanwhile, BITPV with 31.25 % WWR and 50 % cell coverage ratio is found to be the optimum configuration when using high-transparency TPV. Furthermore, this study presents a systematic method for designing BITPV for a multi-story school building in the tropics.

Keywords: BITPV, energy substitution, illuminance, school building, tropics.

Introduction

One of the major challenges in a building's life cycle is energy consumption. Buildings account for 32 % of total global final energy use, 51 % of global energy consumption, and 19 % of greenhouse gas emissions (Berardi, 2017). According to the Energy Information Administration (2022), 20 % of a building's energy consumption is allocated to artificial lighting. This number accounts for a significant portion of the overall building energy consumption. Choosing energy-saving equipment and implementing energy-saving management for lighting can be adopted as a strategy to reduce lighting energy consumption (Shankar et al., 2021). Meanwhile, switching to renewable energy resources is an advantageous strategy to generate clean electrical energy (Gholami and Røstvik, 2020). The Indonesian government has shown concern for energy use by issuing a Mixed-Energy Use Program. This program aims to replace non-renewable energy with renewable energy by up to 25 % by 2025 and 31 % by 2050 (ENERGI INDONESIA 2019 SEKRETARIAT JENDERAL DEWAN ENERGI NASIONAL, 2019). In Indonesia, solar energy is the largest renewable energy resource, with a capacity of 207.8 GWp. The application of BIPV on vertical facades is considered potential and advantageous for optimizing the use of solar energy in the rapid development of urban high-rise buildings in Indonesia. The solar irradiance received might not be as high as that received by the horizontal facade; however, the larger area of the vertical facade is likely to satisfy the building's energy demand.

The vertical facade has the potential to be integrated with photovoltaic (PV) systems and generate clean electrical energy to meet the demand for lighting. The intensive use of energy in school buildings is mostly related to their high occupancy density, lighting power density, and receptacle power density (ASHRAE, 2016; Badan Standarisasi

For citations: Susan, S., Zakaria, S. A., Syed Fadzil, S. F. (2024).
Optimization of the building-integrated transparent photovoltaic configuration based on daylight and energy performance in school buildings in the tropics. Architecture and Engineering, No 1 (9), pp. 29–43. DOI: 10.23968/2500-0055-2024-9-1-29-43.

Nasional, 2000). Hence, the function of the vertical facade ensuring side daylighting cannot be neglected. Side lighting is the most widely used natural lighting system in buildings (Milaningrum, 2015). It is mostly found in the form of a window and has several other functions, such as providing access to outdoor views, natural ventilation, and sound dampening. Daylighting itself is an important element in building design. A well-designed daylighting system can enhance the performance of both buildings and their occupants. In terms of the building's performance, daylighting contributes to reducing the demand for lighting energy. As for the occupants, daylighting will enhance their health, social interaction, psychological well-being, emotions, and visual comfort. In particular, previous studies already found a significant relationship between daylighting and the educational process, especially in school buildings. It was found that students at schools with daylighting performed better and achieved better results than students at schools with artificial illumination. Good daylighting was found to contribute to creating a pleasant environment, enhancing academic performance, and promoting better health (Tsikra and Andreou, 2017).

The technology of transparent PV (TPV) offers the opportunity to meet both needs. For buildings, the extensive development of this technology offers advantages primarily because of its ability to provide clean energy and maintain the function of the building envelope as a daylighting aperture. Previous studies found that the application of PV windows can result in significant energy performance improvements if a high window-to-wall ratio (i.e., ≥45 %) is provided (Sun et al., 2019). However, windows account for a significant amount of heat gain and heat loss (Abbaas et al., 2023). Enlarging windows to install TPV and increase energy production is not a good option in the tropics, where 30–40 % window-to-wall ratio (WWR) is considered the optimum ratio to achieve a balance between energy and lighting. Therefore, it is necessary to find another strategy to optimize the implementation of building-integrated transparent photovoltaic (BITPV) in the tropics. The study proposes an optimization strategy using TPV with different visible transmittance (VT) values based on the spacing between TPV cells on a transparent substrate region. The optimum configuration here is defined as the one that provides an adequate amount of energy production as well as promotes sufficient indoor illumination.

Several previous studies on the use of PV windows or TPV were conducted in mid to high latitude areas, for example in Italy, the US, the UK, and China (Do et al., 2017; Hu et al., 2024; Musameh et al., 2022; Polo López and Sangiorgi, 2014). A study in the UK found the advantages of PV windows in terms of a lower heat transfer coefficient and lower solar heat gain compared to those of transparent single glazing (Alrashidi et al., 2020a). Furthermore, it was found that PV windows can achieve higher net energy savings compared to single-glazed windows (Alrashidi et al., 2020b). An experimental investigation was conducted on PV windows in China, which found that human comfort in a room with a PV window can be achieved when the working surface illuminance ranges between 500–2200 lx (Hu et al., 2024). Other investigation in China found that building shadows have a greater impact on the decrease in power generation and efficiency than the amount of solar radiation received (Xiong et al., 2022). Xuan et al. (2021) proposed the use of concentrator PV to enhance the energy performance of PV windows. The results showed that concentrator PV could enhance the active illumination area by up to 6.69 times. Meanwhile, Fan et al. (2021) attempted to find optimal area ratio-based design strategies for skylight-integrated photovoltaic based on indoor light performance. They considered vertical facade-integrated transparent photovoltaic based on visible transmittance and cell coverage ratio (percentage of PV cells arranged with a certain spacing on a transparent substrate region). The consideration of these two indicators is proposed as a strategy for optimizing tropical BITPV. It is important to conduct measurements not only for daylight performance but also for energy performance. Therefore, two software programs for lighting and energy simulation were used as the tools in the experimental method. The configuration found in this study could be used for the selected building and others that are relevant to the indicated building typologies. Furthermore, the systematic method used in this study can be generalized to design building-integrated transparent photovoltaic in a multi-story school building in the tropics.

Building-Integrated Transparent Photovoltaic (BITPV)

The operation of BITPV depends on several groups of factors: external factors, PV-related factors, and building-related factors. The external factors refer to the amount of solar irradiance. It is known that the intensity of solar radiation is getting less as the latitude of the area is getting higher (McMullan, 2018). Areas with lower latitudes, particularly those in the tropics, receive relatively higher solar irradiance. However, the amount of solar irradiance fluctuates based on several reasons. The average solar irradiance fluctuates around 1353 W/m^2. The amount of solar radiation emitted is different from the amount of solar radiation received. The amount of solar irradiance received represents a combination of direct, diffuse, and reflected solar radiation. The amount received on a vertical plane is also different from the one received on a horizontal plane.

When it comes to PV-related factors, performance will depend on the PV temperature, types of silicon, efficiency, and the number of cells in a module (Lee et al., 2020). The condition in which PV can operate optimally is called Standard Test Condition (STC), which refers to a condition at 25 °C and 1000 W/m^2. However, when PV receives solar radiation, its temperature will increase, and the actual energy output will decrease. The measured difference between the expected energy output and the actual energy output (discrepancy factor) is about 6 %. The PV technology has moved towards transparent photovoltaic, which is industrially known as PV glass, PV window, or transparent PV. This technology allows a certain amount of visible light to transmit into indoor areas. There are several types of technology for creating TPV. One frequently used technology is called selective light transmission. The use of light-transmissive TPV modules on a vertical facade will contribute to generating clean on-site electrical energy for lighting energy demand. Their use will also influence the daylighting performance within the building in terms of providing suitable conditions for visual health and comfort. Fig. 1a shows the light-transmissive PV module application. Here, PV cells are arranged with a certain spacing on a transparent substrate region (Lee et al., 2020). Basically, there are three types of silicon: monocrystalline, polycrystalline, and amorphous silicon. The types of silicon used in TPV influence its efficiency. As is generally known, the crystalline type has higher efficiency compared to the amorphous type. The PV cell here also has a certain VT value. It is developed using c-Si micro-sized PV cells arranged at various densities, ranging from 5.1 to 15.4 cells/cm^2, to adjust the transmittance from 35 to 70 % (as shown in Fig. 1b).

Recently, manufacturers have developed two types of TPV cells: high solar cell density with 15 % VT and low solar cell density with 38 % VT. Higher light transmittance leads to lower TPV efficiency. The efficiency of a PV system can be calculated using the equation below:

$$\text{Efficiency} = \text{output/input} = (V_{mpp} \times I_{mpp}) / (G \times A). \qquad (1)$$

Based on the equation above, the electrical energy output of a PV system can be calculated if the PV efficiency and the input are known. It can be measured by the following equation.

$$\text{Ouput} = \text{efficiency} \times \text{input} = \text{efficiency} \times (G \times A), \qquad (2)$$

where:

V_{mpp} = maximum power point voltage (V);
I_{mpp} = maximum power point current (A);
G = solar radiation intensity (W/m^2);
A = PV area (m^2).

The spacing arrangement between TPV cells impacts the number of PV cells. The greater the spacing, the fewer the number of TPV cells, which means less electrical energy generation as well.

When it comes to building-related factors, the form of the building, shading conditions, tilt and orientation angles, and the available area for PV modules are factors that influence the performance of BITPV. The buildings in the tropics are typically designed to minimize the amount of solar radiation they receive. The shape and layout are usually elongated and shallow in response to this climate (Markus and Morris, 1980). To optimize the performance of BITPV, the building should have relatively low obstruction, so it has less shading from the surroundings and more access to daylight and solar radiation (Al Mamun et al., 2017; Ubisse and Sebitosi, 2009). As a rule of thumb, the tilt of PV panels in building-integrated photovoltaic (BIPV) applications is usually set at the same angle as the geographical latitude. Meanwhile, the south orientation is determined to be the optimal position in terms of visual comfort and energy yield (Mangkuto et al., 2024). The availability of the PV

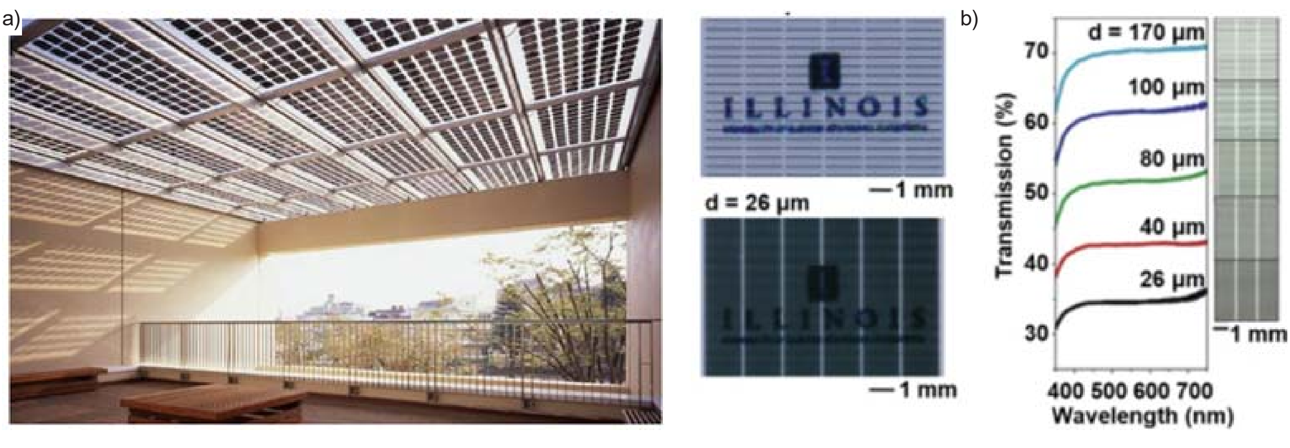

Fig. 1. Light-transmissive TPV modules (Lee et al., 2020; Peng et al., 2011)

area will directly impact the amount of solar radiation received. The larger area means the higher amount of solar radiation received and greater electrical energy generated (Roberts and Guariento, 2009). The available area on a vertical facade depends on the proportion of transparent and opaque materials. Previous studies addressed various ratios of transparent to opaque materials. Nowadays, there is an opportunity for PV to be integrated as a transparent material. Therefore, there is a need to address the ratio of TPV to transparent material (opening). This study addresses BITPV configurations based on VT and the number of TPV cells. VT is influenced by the density of micro-sized PV cells applied, which can be found in the market as low-transparency TPV type and high-transparency TPV type. The number of cells depends on the various spacing ratios of the TPV cells on a transparent substrate region (opening). The studied spacing ratio ranged from 20 to 80 %.

Lighting

Lighting is widely discussed both in terms of daylighting and artificial lighting. Daylight can be introduced into a room through top lighting, side lighting, or combination of both (Lechner, 2014). Since buildings in the tropics receive high solar irradiance, therefore, side lighting seems to be the most preferable strategy to provide natural light without excessive heat. The strategy of daylighting can be divided into four main considerations: site development, external elements, internal elements, and roof and in-wall systems (Ander, 2003; Heerwagen, 2003). When it comes to in-wall systems, the glazing properties, particularly VT, are critical parameters that need to be considered in order to enhance adequate daylight within the building. It represents a fraction of visible light that is transmitted through the glazing system. Higher VT means a greater opportunity for daylight penetration. Light-transmissive TPV modules have opaque PV arranged with specific spacing on a transparent substrate region. The transparent substrate region is usually made of low-E glass, which has a transmittance value of up to 79 %. Meanwhile, the PV cells commonly found in the market have transmittance values of 15 and 38 %. The strategies chosen will influence the quality of daylight within the building. Furthermore, daylight is considered to be of good quality if there is enough natural light between 8:00 am and 4:00 pm (Badan Standarisasi Nasional, 2000). The quality of daylight can be measured by several indicators, including illuminance level (E), useful daylight illuminance (UDI), daylight factor (DF), daylight autonomy (DA), and spatial daylight autonomy (sDA). Regarding these indicators, there are many international standards. However, some countries already have their own national standards (Vardanyan, 2021). In Indonesia, according to Green Building Council Indonesia (GBCI), 300 lux for illuminance level is considered as a good indicator of conditions that provide visual health and comfort for a classroom (Green Building Council Indonesia, 2014; McMullan, 2018).

Since daylighting is very dynamic, artificial lighting is needed as a supplement to daylighting. It is the second biggest building energy consumer after the air conditioning (Kwong and Ali, 2011). To optimize the lighting energy performance, buildings are suggested to use artificial lighting energy-saving equipment (Gandah et al., 2022), while still maintaining the illuminance level standard. As mentioned before, lighting contributes to 20 % of building energy consumption, and the average energy consumption index for buildings in Indonesia is measured at around 240 kWh/m^2 per year (Biantoro and Permana, 2017). Lighting power density (LPD) can be used as a parameter for energy-saving equipment. LPD indicates the amount of lighting power consumption (in watts) per unit area (m^2). This parameter can be used to ensure that the artificial lighting system does not exceed the maximum power density. According to GBCI, the standard for LPD in classrooms is 15 W/m^2. To achieve better lighting energy performance, GBCI determined that LPD should be 20 % less than the standard.

Methods

This study used an experimental method with simulation as its tool. The experiment aimed to find the optimum configuration of BITPV. Optimization is the act of obtaining the best result under given circumstances (Rao, 2009). This means that optimization is the process of finding the conditions that yield the maximum or minimum value of a function. A gradient method is a general optimization strategy that iteratively changes the parameters to increase (or decrease in the case of minimization) the gradient (Sugiyama, 2016). This study aims to analyze the data on illuminance and the percentage of lighting electrical energy substitution for a school building in the tropics. The analysis is based on experimental results obtained from the glazing system, which involved TPV application. The application varied in terms of the spacing between TPV cells and VT of the TPV cells. The constraint is an illuminance level of 300 lux and a substitution percentage of 25–31 % of renewable to non-renewable energy. In this study, lighting energy consumption is measured based on 20 % of the energy consumption index, which is around 240 kWh/m^2 per year. The optimal configuration is defined as the configuration that can reach the constraint optimally.

Research context

The research context is chosen based on several rules of thumb, including the organization of school layout and the typology of buildings in the tropics. Based on previous studies, there are several general organizational layouts for schools.

The central corridor layout with classrooms on its perimeter gives an advantage in terms of optimizing daylight penetration. Commonly, classrooms have several types of proportions, such as 3:2, 2:3, or 1:1 (Montenegro et al., 2012). Meanwhile, due to climate-responsive strategies, buildings in the tropics are usually characterized by (1) an elongated shape and shallow layout, aiming to optimize cross ventilation (Markus and Morris, 1980), as well as (2) the placement of main functional rooms on the building perimeter, aiming to optimize the use of daylight (Heerwagen, 2003). The selected room should be one that is relatively placed on a high floor, has fewer obstructions (Ubisse and Sebitosi, 2009), and has openings on its south orientation (Mangkuto et al., 2024). Furthermore, the selected building should be a multi-story building with the potential for a vertical facade to be integrated with TPV (Xiang and Matusiak, 2022).

Following these general rules of thumb, a school building, namely Universitas Ciputra Surabaya (UCS), was selected as the research context. Fig. 2 shows the site plan and the perspective of UCS. UCS is located at 7°29’ S 112°63’ E. This location itself indicates the potential for solar radiation. This area has a hot and humid climate, with maximum and minimum temperatures ranging around 31.3–35.9 °C and 20.4–23.9 °C, respectively. Meanwhile, the average relative humidity ranges around 65 to 84 %. The highest precipitation mostly occurs from December to February, while September and October appear to be the driest months of the year. The duration of sunshine hours is quite high, reaching 72.27 %. The room being studied is a classroom / drawing studio used by the School of Creative Industry (Fig. 3). The area of the classroom is 192 m^2 with a width of 12 m and a length of 16 m. The floor-to-floor height is 4 m, while the clear height (finished floor to exposed beam) is 3.5 m. The total clear opening width is 17.5 m, and the clear opening height is 2 m. This room has a 112 m^2 exterior wall, with 35 m^2 being the opening. The building’s response to the surrounding climate is demonstrated by its 31.25 % window-to-wall ratio (WWR), which falls within the preferred range for buildings in tropical regions. Fig. 3 shows the layout of the room selected.

Experimental setting

The experimental method is chosen to discover the impact of the VT value, as well as cell numbers, as a result of the TPV ratio arrangement on a transparent substrate region (opening). The experimental method requires three stages: a pre-test condition, treatment, and a post-test condition. Table 1 shows the experimental method settings, while Table 2 shows the TPV ratio settings for the opening of the building’s vertical facade.

Following the experimental method, simulations were chosen as a tool to generate data on illuminance levels and solar radiation received in each configuration. Velux was used to generate data on illuminance levels, and the simulation was run for several time periods (09:00, 12:00, 16:00) to validate the feasibility of the experimental method and procedure. As for the data on solar radiation received, Archipak was used, followed by mathematical calculations to measure the electrical energy generation. A gradient diagram was used to determine the optimum configuration of BITPV, which is defined as the one that has the optimum illuminance level and substitutes a minimum of 25–31 % of conventional lighting energy with the electrical energy generated from PV. The optimization workflow is shown in Fig. 4.

Fig. 2. Site plan and perspective of Universitas Ciputra Surabaya

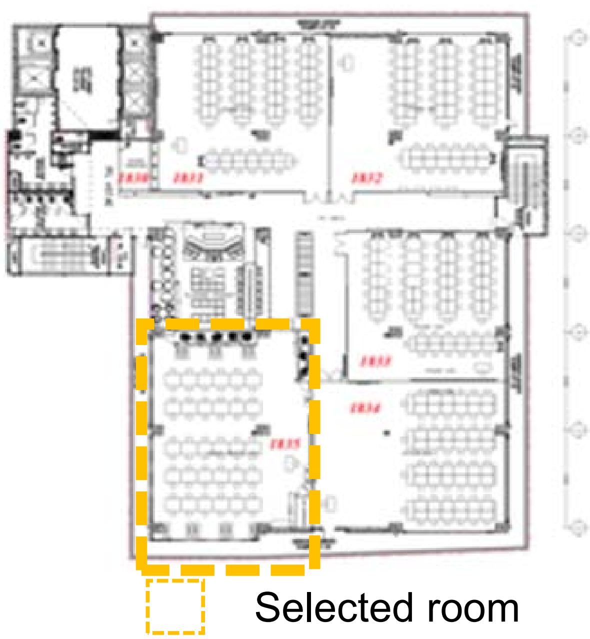

Fig. 3. Layout of the room selected

VELUX simulation: validation and setting

A previous study showed that simulation results matched well with the results obtained from field measurements (Kousalyadevi and Lavanya, 2019). The reliability of Velux results was also confirmed by another previous study conducted by Xiang and Matusiak (2022). In that study, Velux was employed to find a balance of daylight on a colored facade-integrated photovoltaic design for a high-rise building with balconies. It mentioned the following advantages of Velux software: the most architect-friendly software, a satisfying general interface and graphic treatment of results, accurate prediction of daylight levels and the appearance of a daylit area. Furthermore, Velux was chosen because it is known as software that has the ability to generate automated reports with user-defined daylight measurement zones (work planes). It is validated in accordance with the CIE 171:2006 test cases to assess the accuracy of lighting computer programs (Labayrade et al., 2009). However, to increase accuracy and reliability, it is suggested that simulated results be validated by measured results (Wong, 2017). The illuminance value and illuminance distribution pattern can be used to determine whether the model is able to generate realistic data (Lakhdari et al., 2021). It is assumed that the simulation result matches well with the measurement result if the difference is less than 4 % (Sun et al., 2019). Therefore, measurements and simulations under base case conditions are conducted to generate data on illuminance values and their distribution patterns. The measurements were conducted in grids of 1.20 ×1.20 m, resulting in 134 measured points. An example of a measurement result, particularly in April at 12:00, is shown in Table 2. Meanwhile, the simulation resulted in 42 simulated points, as shown in Table 3. The distribution patterns for the measured and simulated results are illustrated

Table 1. **Experimental method**

Pre-test	Treatment	Post-test
A model classroom in a tropical, multi-story school building with an active system that has optimal solar access	BITPV configuration based on PV with different VT: PV1 = low transparency (15 % VT, 38 Wp/m², 16 % efficiency) PV2 = high transparency (38 % VT, 22 Wp/m², 9.3 % efficiency) BITPV configuration based on PV with different cell numbers, as a result of the ratio arrangement of transparent PV to transparent substrate (20 %, 30 %, ..., 80 %)	Various configuration of glass cladding-BIPV: 1. 20 % - PV1 2. 20 % - PV2 3. 30 % - PV1 4. 30 % - PV2 5. 40 % - PV1 6. 40 % - PV2 7. … 8. … 9. …

Table 2. **Setting of the TPV to Opening Ratio**

Treatment code		Window area (m^2)		TPV area (m^2)	
		S	W	S	W
0 % (base case)		11	24	0	0
20 % - PV1	20 % - PV2	11	24	2.244	5.000
30 % - PV1	30 % - PV2	11	24	3.366	7.272
40 % - PV1	40 % - PV2	11	24	4.555	9.792
50 % - PV1	50 % - PV2	11	24	5.466	12.600
60 % - PV1	60 % - PV2	11	24	6.722	14.712
70 % - PV1	70 % - PV2	11	24	7.844	16.656
80% - PV1	80% - PV2	11	24	8.822	19.032

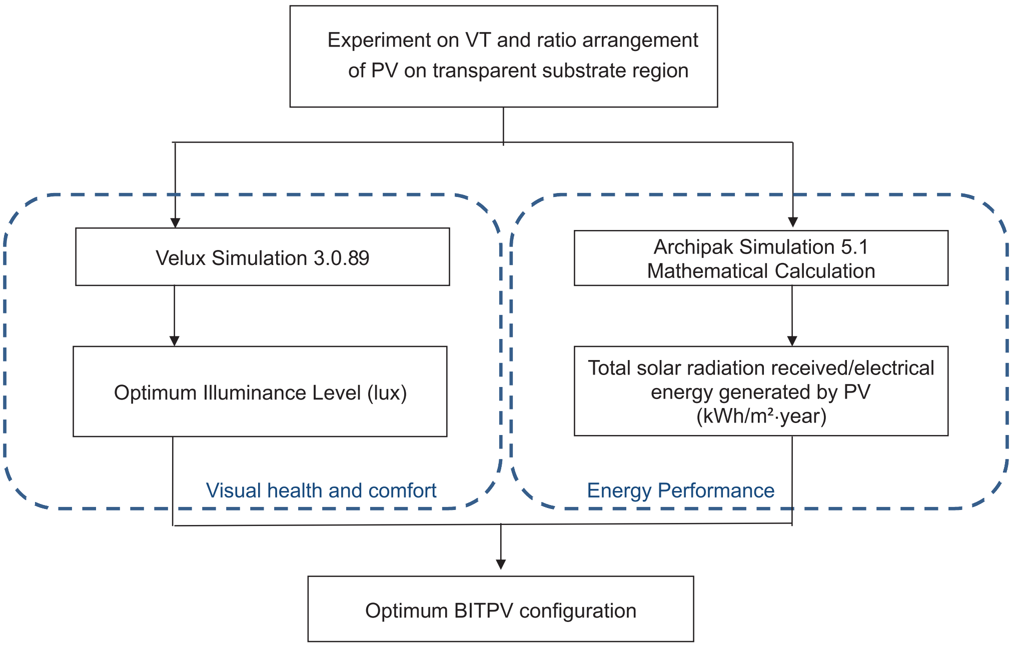

Fig. 4. Optimization workflow

in Fig. 5. The difference in average illuminance, which ranges from 0.58 to 3.72 %, and the similarity in distribution patterns indicate the reliability of the simulation.

The materials and finishes for each room element are shown in Table 4. PV is set as another customized material, with a glass surface and two options for transmittance: 15 % (PV1) and 38 % (PV2). The location is customized based on the building's longitude (112°63' E) and latitude (7°29' S). Other settings include the camera, which is set to perspective for still images; the render type, which is set to illuminance; overcast sky conditions; a year-long time frame; and several times of the day, including 09:00, 12:00, and 16:00. The Velux simulation was run 540 times (15 models × × 12 months × 3 times).

ARCHIPAK simulation setting

Archipak is a software developed by Szokolay and validated through comparison with other software, namely TEMPER, CHEETAH, and QUICK, as well as through comparison of simulation results and measured data (Ahmad and Szokolay, 1993; Szokolay, 1986). It is an integrated program for thermal and solar radiation that was used in several previous studies. In some recent studies, Archipak was described as a digital architecture tool that specifically helps users in simulating physical building needs (Andadari et al., 2021). It is used to determine comfort zones and control potential zones (Rabah and Tamakan, 2002), as well as to calculate solar radiation, annual cooling, and overheating energy (Noerwasito and Nirwansyah, 2019; Noerwasito, 2022; Susan and Wardhani, 2020a, 2020b). In this study, Archipak was used to generate data on the solar radiation received at a determined orientation and tilt angle. The simulation settings on Archipak consist of location and climatic data input, retrieving climatic data for simulating solar radiation received, and setting data output for an average day of 12 months. This is for an area with a 90° tilt angle from the horizon (vertical facade), oriented at 180° and 270°. Previous studies showed that the predicted data of PV energy output matches well with the measured data when the measured solar radiation data is used as input to the simulation software (Wu et al., 2015; Andadari et al., 2021). Therefore, climatic data for Surabaya derived from *Badan Meteorologi and Geofisika Juanda* was used as the input for climatic data. The climatic data is listed in Table 5. To enhance reliability, a 10–30 % reduction in every shading condition (Feng et al., 2023; Ubisse and Sebitosi, 2009; Zomer and Rüther, 2017), as well as a 1–6 % discrepancy factor (Trinuruk et al., 2009; Wu et al., 2015), were taken into account in the power output calculation.

Results and discussion

As shown in the workflow in Fig. 4, simulations using Velux were applied after setting up the experiment on VT and the ratio arrangement of PV on the transparent substrate region (Table 2). Every model was simulated in Velux for 12 months, three times a day. The simulation output in the form of images displays data from 42 points measuring illuminance. This data will include information about the location, time, orientation, sky conditions, and external illumination. For every simulation output, the levels of illuminance are observed in terms of minimum (E_{min}), maximum (E_{max}), and average (E_{avg}) values. For example, in the base case model,

Table 2. **Measured results (lux)**

Grid No.	1	2	3	4	5	6	7	8	9	10	Total	Average illuminance
1	281	882						52	14		1229	
2	310	765	64	49	37	27	20	9	14		1295	
3	572	882	173	82	49	37	27	14	14		1850	
4	572	281	173	107	49	49	27	20	27		1305	
5	572	445	173	136	49	37	37	49	82	354	1934	
6	572	281	173	128	49	49	37	49	64	445	1847	
7	572	281	136	107	49	49	281	173	27	445	2120	
8	572	173	136	107	64	64	56	82	27	572	1853	
9	959	218	218	107	64	64	54	54	82	354	2174	
10	959	281	281	281	82	82	37	107	107	354	2571	
11	959	281	281	173	107	107	82	59	82	354	2485	
12	3398	445	354	281	173	173	107	49	49	445	5474	
13	2256	218	218	136	107	107	218	107			3367	
14	2121	354	173	173	107	107	173	281			3489	
15	354	1559	1114	882	572	572	1211				6264	
											39257	292.96

Table 3. **Simulated results (lux)**

Grid No.	1	2	3	4	5	6	7	Total	Average illuminance
1	159.1	176.3	180.1	190.5	138.4	49.2	237.3	1130.9	
2	185.2	132.4	62.7	81.7	331.1	290.1	76.1	1159.3	
3	192.9	188.7	252.2	254.8	219.1	0	148.9	1256.6	
4	337.4	260.5	418.6	595.6	303.8	0	181.8	2097.7	
5	489.8	499.2	585.5	619.5	725.0	723.2	151.4	3793.6	
6	332.5	348.6	337.5	423.0	429.7	510.0	557.1	2938.4	
								12.376.5	294.68

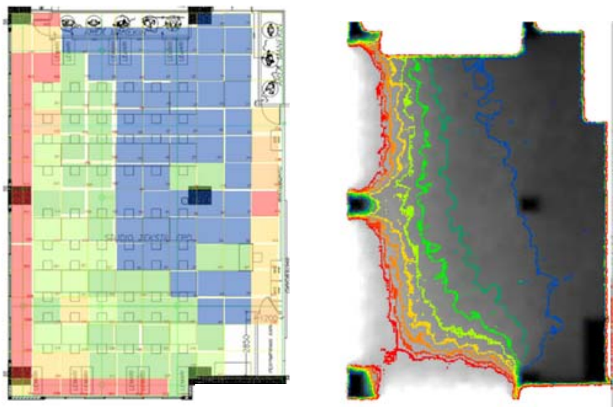

Fig. 5. Distribution patterns of (a) measured results and (b) simulated results

simulations in March, June, September, and December at 12:00 resulted in illuminance value ranges of 51.4–771.6 lux, 44.1–650 lux, 49.8–855.8 lux, and 49.6–727.9 lux, respectively. In this case, the average illuminance value calculated from every 42 points of measuring illuminance is 303.8 lux, 262.5 lux, 303.8 lux, and 290.6 lux, respectively for March, June, September, and December. Another example is for the model of 30 % - PV1. The illuminance value ranges are 34.5–826 lux, 27.6–736.6 lux, 38.1–751.6 lux, 39.4–813.4 lux. The average illuminance values for the four consecutive months mentioned before are 213.1 lux, 184.5 lux, 179.9 lux, and 210.7 lux, respectively. The annual average illuminance results are shown in Table 5.

Table 4. **Room material and finishing settings**

Element	Material	Thickness	Color	Transmittance	Reflectance	Specularity	Roughness
Ceiling	Concrete	-	White matte	-	0.94	0.05	0.01
Wall	Hebel	-	Light gray	-	0.71	0.05	0.01
Opening	Low-E glass	12 mm	Clear	0.71	0.043	-	-
Framing	Aluminum	-	Black matte	-	-	0	0.1
Floor	Ceramic	-	Gray-glossy	-	0.58	0.05	0.3

The monthly maximum average illuminance, particularly for September (equinox), is shown in Table 6. The annual and monthly average illuminance will be used for optimization considerations.

The Archipak simulation was run to generate data on solar radiation received. For vertical facade facing 180° and 270° orientations, the amount of solar radiation received is 1777 kWh/m² per year and 2213 kWh/m² per year, respectively. As mentioned earlier, the selected classroom has an area of 192 m^2 and an energy consumption index of 240 kWh/m^2 per year. With 20 % of the energy consumption allocated to lighting, the total energy demand for the selected class is 9216 kWh per year. Based on this energy demand, mathematical equations were used to calculate the percentage of renewable energy substitution as a parameter for lighting energy performance. The calculation is shown in Table 7.

The data on the illuminance level and energy performance is then plotted on the gradient diagram. It was found that the annual average illuminance dropped below the standard. Based on this result, the optimum configuration is determined as a configuration with an annual illuminance level that is closest to the standard and has energy substitution within 25–31 %. The monthly maximum average illuminance is also analyzed and used to support the determination of the optimum configuration, which is defined as the configuration with monthly maximum average illuminance ranging within 300 lux and having energy substitution within 25–31 %. Figs. 6 and 7 show the gradient diagram for the optimization process.

Conclusion

This study aimed to find the optimum configuration of BITPV for a school building in the tropics. A site was selected based on its typology

Table 5. **Overall average illuminance value**

Treatment code	Overall average illuminance value in every month (lux)										
	Jan	Feb	Mar	Apr	May	Jun	Jul	Oct	Nov	Dec	Avg
Base case	220.0	223.85	225.3	216.8	202.4	190.9	191.6	218.2	227.8	238.9	224.6
20 % - PV1	169.3	171.5	161.8	159.9	148.7	140.7	146.9	149.9	155.0	166.8	166.6
30 % - PV1	156.1	158.9	157.6	152.2	141.6	134.0	134.1	143.0	133.2	157.7	156.6
40 % - PV1	146.7	145.3	145.7	140.1	133.5	124.2	123.5	130.7	122.5	145.2	145.2
50 % - PV1	123.9	129.7	123.1	116.2	109.1	118.9	119.4	124.7	111.3	140.3	141.5
60 % - PV1	109.4	112.1	113.2	107.6	100.4	98.8	99.1	101.7	100.8	111.2	111.3
70 % - PV1	100.8	102.1	101.6	103.9	99.6	95.0	95.0	102.1	94.0	107.2	101.3
80 % - PV1	80.5	86.3	90.0	93.8	91.7	85.4	86.6	93.5	84.0	89.9	84.2
20 % - PV2	193.1	195.7	195.6	188.5	175.7	169.8	166.8	176.4	163.2	194.8	196.0
30 % - PV2	163.9	159.8	159.6	154.9	155.6	135.9	135.7	143.9	147.9	160.3	158.6
40 % - PV2	153.0	149.1	149.9	143.4	143.1	126.2	129.6	136.8	145.3	151.5	150.1
50 % - PV2	137.9	140.5	140.3	135.1	130.0	103.0	127.5	134.8	136.2	149.6	148.8
60 % - PV2	113.2	116.0	116.8	111.7	104.6	99.2	100.0	105.4	108.5	116.2	115.9
70 % - PV2	109.4	111.5	112.7	109.3	100.7	95.4	97.6	105.4	101.5	112.6	111.5
80 % - PV2	86.7	92.7	99.9	102.4	93.6	92.6	95.2	95.0	92.9	97.4	91.5

Table 6. **Average maximum illuminance in September**

Treatment code	E_{max} at 09:00 (lux)	E_{max} at 12:00 (lux)	E_{max} at 16:00 (lux)	Avg of E_{max} (lux)
Base case	693.7	855.8	492.0	680.5
20 % - PV1	575.3	805.6	405.2	595.4
30 % - PV1	523.6	751.6	370.6	548.6
40 % - PV1	397.8	594.0	304.6	432.1
50 % - PV1	340.3	502.0	249.0	363.8
60 % - PV1	280.3	406.4	207.1	297.9
70 % - PV1	261.1	384.4	200.5	282.0
80 % - PV1	225.2	331.4	186.8	247.8
20 % - PV2	603.5	727.3	425.5	603.5
30 % - PV2	600.8	719.8	427.9	600.8
40 % - PV2	490.0	629.9	306.8	490.0
50 % - PV2	462.0	550.5	302.1	462.0
60 % - PV2	374.4	511.2	247.4	374.4
70 % - PV2	332.1	469.0	241.6	332.1
80 % - PV2	223.4	304.4	152.3	223.4

Table 7. **Lighting energy performance**

Code	Window area (m²)		PV area (m²)		PV area (%)		Electrical energy generation: Annual rad rec. (kWh/m² per year) before shading		Annual rad rec. (kWh/m² per year) after shading		Total annual rad rec. (kWh per year)	PV eff. (%)	Disc. factor (%)	Electrical energy generated (kWh per year)	Percentage of substitution
	S	W	S	W	S	W	S	W	S	W					
	(a)	(b)	(c)	(d)	(e)	(f)	(g)	(h)	(i)	(j)	(k) = (cxi)+(dxj)	(l)	(m)	(n) = (k) × (l) − (m)	(k) = (n)/9216 × 100%
0 % - base case	11	24	0	0	0	0	1777	2213	1243.9	1549.1	0	16	6	0	0
20 % - PV1	11	24	2.244	5.000	20.4	20.8	1777	2213	1243.9	1549.1	10536.81	16	6	1685.83	18
30 % - PV1	11	24	3.366	7.272	30.5	30.3	1777	2213	1243.9	1549.1	15452.02	16	6	2472.26	27
40 % - PV1	11	24	4.555	9.792	41.4	40.8	1777	2213	1243.9	1549.1	20834.75	16	6	3333.50	36
50 % - PV1	11	24	5.466	12.600	49.6	52.5	1777	2213	1243.9	1549.1	26317.82	16	6	4210.79	46
60 % - PV1	11	24	6.722	14.712	61.1	61.3	1777	2213	1243.9	1549.1	31151.86	16	6	4984.24	54
70 % - PV1	11	24	7.844	16.656	71.3	69.4	1777	2213	1243.9	1549.1	35558.96	16	6	5689.37	62
80 % - PV1	11	24	8.822	19.032	80.2	79.3	1777	2213	1243.9	1549.1	40456.16	16	6	6472.93	70
20 % - PV2	11	24	2.244	5.000	20.4	20.8	1777	2213	1243.9	1549.1	10536.81	9.3	6	979.86	11
30 % - PV2	11	24	3.366	7.272	30.5	30.3	1777	2213	1243.9	1549.1	15452.02	9.3	6	1436.98	16
40 % - PV2	11	24	4.555	9.792	41.4	40.8	1777	2213	1243.9	1549.1	20834.75	9.3	6	1937.57	21
50 % - PV2	11	24	5.466	12.600	49.6	52.5	1777	2213	1243.9	1549.1	26317.82	9.3	6	2447.50	27
60 % - PV2	11	24	6.722	14.712	61.1	61.3	1777	2213	1243.9	1549.1	31151.86	9.3	6	2897.06	31
70 % - PV2	11	24	7.844	16.656	71.3	69.4	1777	2213	1243.9	1549.1	35558.96	9.3	6	3306.92	36
80 % - PV2	11	24	8.822	19.032	80.2	79.3	1777	2213	1243.9	1549.1	40456.16	9.3	6	3762.36	41

that conforms to general school organization, is responsive to tropical climate, and has the potential to be integrated with BITPV. Treatments based on different VT and cell numbers were applied to the selected site, which functioned as the base case or pre-test model. The variation in VT is a result of the micro-sized PV density arrangement, while the number of cells is a result of the various spacing between PV cells in a module. Data generated from the simulation shows the levels of illuminance and energy generation for several post-test models. It was found that the annual average illuminance for both the pre-test and post-test models falls below the standard. The annual average illuminance for the pre-test model, which has 31.25 % WWR, is 224.6 lux. The level of illuminance drops within a range of 27–59 % for BITPV with low-transparency PV, and 15–56 % for BITPV with high-transparency PV. However, considering energy substitution as a parameter for optimization, configurations of 30 % PV1 and 50 % PV2 can be proposed as the optimum BITPV. These configurations result in an annual average illuminance that is closest to the standard while still maintaining an energy substitution percentage of 27 %.

However, if we consider the maximum illuminance value, the average ranges from 223.4 lux to 680.5 lux. Based on the maximum illuminance value and energy substitution, there are three configurations that can comply with the optimization standard. These are 30 % PV1, 50 % PV2, and 60 % PV2. These configurations can provide a monthly maximum average illuminance above the standard (548.6 lux, 438.2 lux, and 377.7 lux, respectively), while still maintaining percentages of energy substitution within the range of 25–31 %. Furthermore, this study presented a systematic method to design building-integrated transparent photovoltaic in a multi-story school building in the tropics (as shown in Fig. 8). It started with site selection, building and room geometry, daylight simulation for several selections of TPV cell coverage ratio and visual transmittance, and continued with solar radiation simulation, which was then used to determine the optimal BITPV configuration. Using this approach, indoor daylighting and energy performance can be well optimized.

Daylighting and energy performance in this study are based on simulated data. Actual daylighting and energy performance can be monitored in future research using full-scale physical samples, following the development of TPV technology as well.

Acknowledgments

The research was conducted with Dr. Safial Aqbar bin Zakaria and Dr. Sharifah Fairuz Syed Mohd Fadzil from the School of Housing, Building, and Planning at Universiti Sains Malaysia. This research was funded by Universitas Ciputra Surabaya.

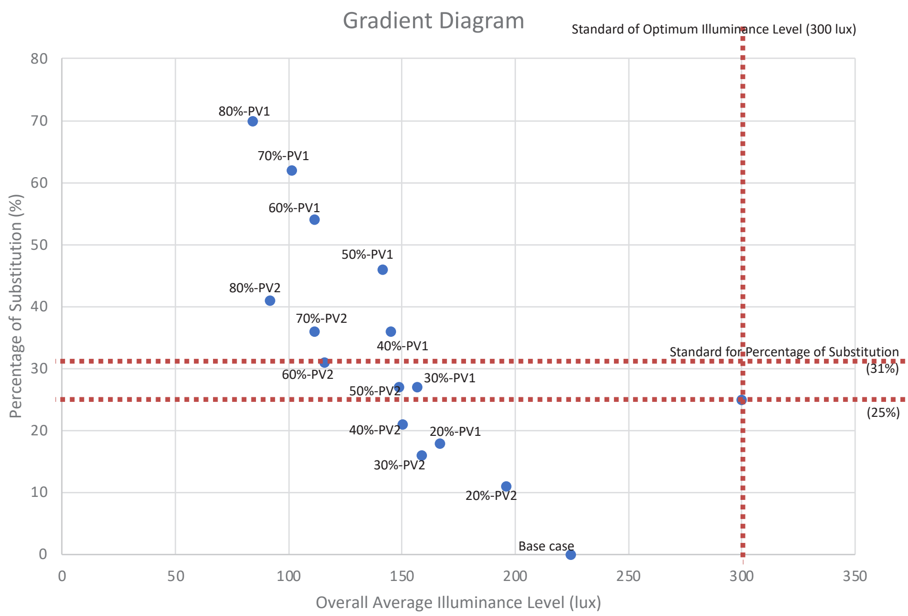

Fig. 6. Optimization diagram based on annual average illuminance and annual energy substitution

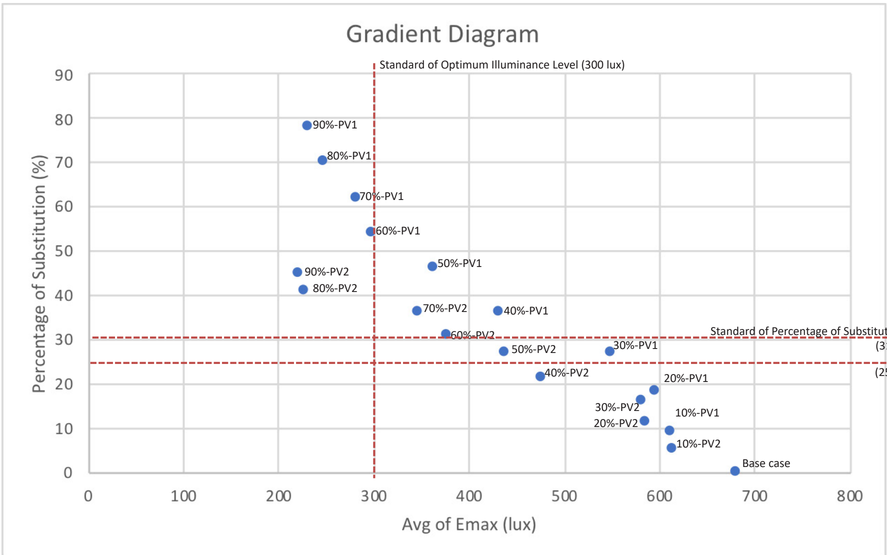

Fig. 7. Gradient diagram based on monthly maximum average illuminance and annual energy substitution

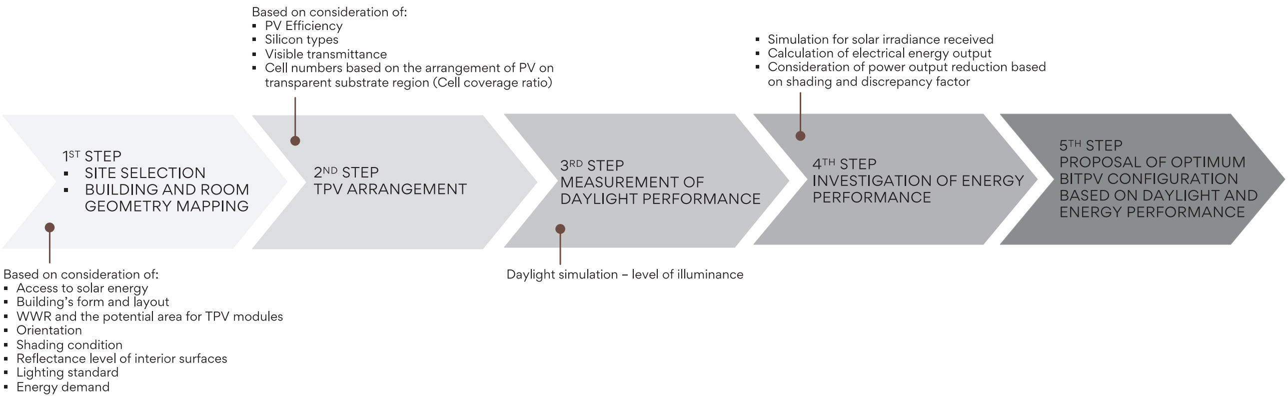

Fig. 8. Systematic method to design BITPV

References

Abbaas, E. S., Ismail, M., Saif, A. A., and Ghazali, M. A. (2023). Impact of window shading on the thermal performance of residential buildings of different forms in Jordan. *Architecture and Engineering*, Vol. 8, No. 1, pp. 25–36. DOI: 10.23968/2500-0055-2023-8-1-25-36.

Ahmad, Q. T. and Szokolay, S. V (1993). Thermal design tools in Australia: A comparative study of TEMPER, CHEETAH, ARCHIPAK and QUICK. In: *Proceedings of the IBPSA Building Simulation Conference*, August 16–18, 1993, Adelaide, SA, Australia. Vol. 93, pp. 351–357.

Al Mamun, M. A., Hasanuzzaman, M., and Selvaraj, J. (2017). Experimental investigation of the effect of partial shading on photovoltaic performance. *IET Renewable Power Generation*, Vol. 11, Issue 7, pp. 912–921. DOI: 10.1049/iet-rpg.2016.0902.

Alrashidi, H., Ghosh, A., Issa, W., Sellami, N., Mallick, T. K., and Sundaram, S. (2020a). Thermal performance of semitransparent CdTe BIPV window at temperate climate. *Solar Energy*, Vol. 195, pp. 536–543. DOI: 10.1016/j.solener.2019.11.084.

Alrashidi, H., Issa, W., Sellami, N., Ghosh, A., Mallick, T. K., and Sundaram, S. (2020b). Performance assessment of cadmium telluride-based semi-transparent glazing for power saving in façade buildings. *Energy and Buildings*, Vol. 215, 109585. DOI: 10.1016/j.enbuild.2019.109585.

Andadari, T. S., Purwanto, L. M. F., Satwiko, P., and Sanjaya, R. (2021). Study of digital architecture technology: theory and development. *Journal of Architectural Research and Education*, Vol. 3, No. 1, pp. 14–21. DOI: 10.17509/jare.v3i1.30500.

Ander, G. D. (2003). *Daylighting performance and design*. 2nd edition. Hoboken: John Wiley & Sons, 336 p.

ASHRAE (2016). *Standard 90.1. User's manual*. ASHRAE, Atlanta, GA 30329, USA, 478 p.

Badan Standarisasi Nasional (2000). *Prosedur audit energi pada bangunan gedung. SNI 03-6196-2000*. Badan Standarisasi Nasional, Jakarta, 13 p.

Berardi, U. (2017). A cross-country comparison of the building energy consumptions and their trends. *Resources, Conservation and Recycling*, Vol. 123, pp. 230–241. DOI: 10.1016/j.resconrec.2016.03.014.

Biantoro, A. W. and Permana, D. S. (2017). Analisis Audit Energi untuk Pencapaian Efisiensi Energi di Gedung AB, Kabupaten Tangerang, Banten. *Jurnal Teknik Mesin*, Vol. 6, No. 2, pp. 85–93. DOI: 10.22441/jtm.v6i2.1186.

Do, S. L., Shin, M., Baltazar, J.-C., and Kim, J. (2017). Energy benefits from semi-transparent BIPV window and daylight-dimming systems for IECC code-compliance residential buildings in hot and humid climates. *Solar Energy*, Vol. 155, pp. 291–303. DOI: 10.1016/j.solener.2017.06.039.

ENERGI INDONESIA 2019 SEKRETARIAT JENDERAL DEWAN ENERGI NASIONAL (2019). Available at: https://www.esdm.go.id/assets/media/content/content-indonesia-energy-outlook-2019-english-version.pdf (Date accessed: 1 December 2022).

Energy Information Administration (2022). *Annual Energy Outlook 2022. Electricity*. [online] Available at: https://www.eia.gov/outlooks/archive/aeo22/narrative/electricity/sub-topic-01.php [Date accessed 20 December 2022].

Fan, Z., Yang, Z., and Yang, L. (2021). Daylight performance assessment of atrium skylight with integrated semi-transparent photovoltaic for different climate zones in China. *Building and Environment*, Vol. 190, 107299. DOI: 10.1016/j.buildenv.2020.107299.

Feng, X., Ma, T., Yamaguchi, Y., Peng, J., Dai, Y., and Ji, D. (2023). Potential of residential building integrated photovoltaic systems in different regions of China. *Energy for Sustainable Development*, Vol. 72, pp. 19–32. DOI: 10.1016/j.esd.2022.11.006.

Gandah, F., Al-Adayleh, M., and Al-Ruwaishedi, M. R. (2022). Adopting smart building concept in historical building: case of Abu Jaber museum, Jordan. *Architecture and Engineering*, Vol. 7, No. 3, pp. 3–12. DOI: 10.23968/2500-0055-2022-7-3-03-12.

Gholami, H. and Røstvik, H. N. (2020). Economic analysis of BIPV systems as a building envelope material for building skins in Europe. *Energy*, Vol. 204, 117931. DOI: 10.1016/j.energy.2020.117931.

Green Building Council Indonesia (2014). *GREENSHIP rating tools. GREENSHIP existing building. Version 1.1*. [online] Available at: https://gbcindonesia.org/files/resource/093ec9dc-9f1d-47e3-805a-07887b8c4d81/Summary%20GREENSHIP%20Existing%20Building%20V1.1.pdf [Date accessed 24 October 2022].

Heerwagen, D. (2003). *Passive and active environmental controls: informing the schematic designing of buildings*. New York: McGraw-Hill Science/Engineering/Math, 940 p.

Hu, Y., Xue, Q., Wang, H., Zou, P., Yang, J., Chen, S., and Cheng, Y. (2024). Experimental investigation on indoor daylight environment of building with Cadmium Telluride photovoltaic window. *Energy and Built Environment*, Vol. 5, Issue 3, pp. 404–413. DOI: 10.1016/j.enbenv.2023.01.001.

Kousalyadevi, G. and Lavanya, G. (2019). Optimal investigation of daylighting and energy efficiency in industrial building using energy-efficient velux daylighting simulation. *Journal of Asian Architecture and Building Engineering*, Vol. 18, Issue 4, pp. 271–284. DOI: 10.1080/13467581.2019.1618860.

Kwong, Q. J. and Ali, Y. (2011). A review of energy efficiency potentials in tropical buildings – Perspective of enclosed common areas. *Renewable and Sustainable Energy Reviews*, Vol. 15, Issue 9, pp. 4548–4553. DOI: 10.1016/j.rser.2011.07.097.

Labayrade, R., Jensen, H. W., and Jensen, C. (2009). Validation of Velux Daylight Visualizer 2 against CIE 171:2006 test cases. In: *Building Simulation 2009. Eleventh International IBPSA Conference,* July 27–30, 2009. Glasgow, Scotland, pp. 1506–1513.

Lakhdari, K., Sriti, L., and Painter, B. (2021). Parametric optimization of daylight, thermal and energy performance of middle school classrooms, case of hot and dry regions. *Building and Environment*, Vol. 204, 108173. DOI: 10.1016/j.buildenv.2021.108173.

Lechner, N. M. (2014). *Heating, cooling, lighting: Sustainable design methods for architects.* 4th edition. Hoboken: John Wiley & Sons, 720 p.

Lee, K., Um, H.-D., Choi, D., Park, J., Kim, N., Kim, H., and Seo, K. (2020). The development of transparent photovoltaics. *Cell Reports Physical Science*, Vol. 1, Issue 8, 100143. DOI: 10.1016/j.xcrp.2020.100143.

Mangkuto, R. A., Tresna, D. N. A. T., Hermawan, I. M., Pradipta, J., Jamala, N., Paramita, B., and Atthaillah (2024). Experiment and simulation to determine the optimum orientation of building-integrated photovoltaic on tropical building façades considering annual daylight performance and energy yield. *Energy and Built Environment*, Vol. 5, Issue 3, pp. 414–425. DOI: 10.1016/j.enbenv.2023.01.002.

Markus, T. A. and Morris, E. N. (1980). *Buildings, climate, and energy*. 2nd edition. London: Pitman Publishing Limited, 540 p.

McMullan, R. (2018). *Environmental science in building*. 8th edition. London: Palgrave, 399 p.

Milaningrum, T. H. (2015). Optimalisasi Pencahayaan Alami dalam Efisiensi Energi di Perpustakaan UGM. In: *Prosiding Seminar Topik Khusus/ Juli 2015*.

Montenegro, E., Potvin, A., and Demers, C. (2012). Impact of school building typologies on visual, thermal and energy performances. In: *PLEA2012 - 28th Conference, Opportunities, Limits & Needs Towards an Environmentally Responsible Architecture*, November 7–9, 2012, Lima, Peru. DOI: 10.13140/2.1.3557.5363.

Musameh, H., Alrashidi, H., Al-Neami, F., and Issa, W. (2022). Energy performance analytical review of semi-transparent photovoltaics glazing in the United Kingdom. *Journal of Building Engineering*, Vol. 54, 104686. DOI: 10.1016/j.jobe.2022.104686.

Noerwasito, V. T. (2022). Sawdust and soil block as wall in simple buildings to gain the optimum heat and embodied energy in humid tropical area. *IOP Conference Series: Earth and Environmental Science*, Vol. 1007, 012002. DOI: 10.1088/1755-1315/1007/1/012002.

Noerwasito, V. T. and Nirwansyah, R. (2019). Simple energy-efficient house wall material selection in a humid tropical area — case study in Surabaya. *Advances in Engineering Research,* Vol. 156, pp. 52–55.

Peng, C., Huang, Y., and Wu, Z. (2011). Building-integrated photovoltaics (BIPV) in architectural design in China. *Energy and Buildings*, Vol. 43, Issue 12, pp. 3592–3598. DOI: 10.1016/j.enbuild.2011.09.032.

Polo López, C. S. and Sangiorgi, M. (2014). Comparison assessment of BIPV façade semi-transparent modules: Further insights on human comfort conditions. *Energy Procedia*, Vol. 48, pp. 1419–1428. DOI: 10.1016/j.egypro.2014.02.160.

Rabah, K. and Tamakan, Z. (2002). Application of ARCHIPAK for development of passive solar energy-efficient building in North Cyprus. *Architectural Science Review*, Vol. 45, Issue 3, pp. 219–229. DOI: 10.1080/00038628.2002.9697513.

Rao, S. S. (2009). *Engineering optimization: theory and practice.* 4th edition. Hoboken: John Wiley & Sons, 813 p.

Roberts, S. and Guariento, N. (2009) *Building integrated photovoltaics: a handbook*. Basel: Walter de Gruyter, 192 p.

Shankar, A., Vijayakumar, K., and Babu, B. C. (2021). Energy saving potential through artificial lighting system in PV integrated smart buildings. *Journal of Building Engineering*, Vol. 43, 103080. DOI: 10.1016/j.jobe.2021.103080.

Sugiyama, M. (2016). *Introduction to statistical machine learning*. Waltham, MA 02451 USA: Elsevier, 534 p. DOI: 10.1016/C2014-0-01992-2.

Sun, Y., Shanks, K., Baig, H., Zhang, W., Hao, X., Li, Y., He, B., Wilson, R., Liu, H., Sundaram, S., Zhang, J., Xie, L., Mallic, T., and Wu, Y. (2019). Integrated CdTe PV glazing into windows: energy and daylight performance for different window-to-wall ratio. *Energy Procedia*, Vol. 158, pp. 3014–3019. DOI: 10.1016/j.egypro.2019.01.976.

Susan, S. and Wardhani, D. (2020a). Building integrated photovoltaic as GREENSHIP'S on site renewable energy tool. *Results in Engineering*, Vol. 7, 100153. DOI: 10.1016/j.rineng.2020.100153.

Susan, S. and Wardhani, D. K. (2020b). Photovoltaic and wind turbine: a comparison as building integrated renewable energy in Indonesia. *Humaniora*, Vol. 11, No. 1, pp. 51–57. DOI: 10.21512/humaniora.v11i1.6294.

Szokolay, S. V. (1986). ARCHIPAK an integrated design tool for small solar buildings. *Intersol Eighty Five. Proceedings of the Ninth Biennial Congress of the International Solar Energy Society*, pp. 379–383. DOI: 10.1016/B978-0-08-033177-5.50080-6.

Trinuruk, P., Sorapipatana, C., and Chenvidhya, D. (2009). Estimating operating cell temperature of BIPV modules in Thailand. *Renewable Energy*, Vol. 34, Issue 11, pp. 2515–2523. DOI: 10.1016/j.renene.2009.02.027.

Tsikra, P. and Andreou, E. (2017). Investigation of the energy saving potential in existing school buildings in Greece. The role of shading and daylight strategies in visual comfort and energy saving. *Procedia Environmental Sciences*, Vol. 38, pp. 204–211. DOI: 10.1016/j.proenv.2017.03.107.

Ubisse, A. and Sebitosi, A. (2009). A new topology to mitigate the effect of shading for small photovoltaic installations in rural sub-Saharan Africa. *Energy Conversion and Management*, Vol. 50, Issue 7, pp. 1797–1801. DOI: 10.1016/j.enconman.2009.03.016.

Vardanyan, E. (2021). Sustainability in the process of development permit acquisition (Armenia). *Architecture and Engineering*, Vol. 6, No. 3, pp. 62–69. DOI: 10.23968/2500-0055-2021-6-3-62-69.

Wong, I. L. (2017). A review of daylighting design and implementation in buildings. *Renewable and Sustainable Energy Reviews*, Vol. 74, pp. 959–968. DOI: 10.1016/j.rser.2017.03.061.

Wu, X., Liu, Y., Xu, J., Lei, W., Si, X., Du, W., Zhao, C., Zhong, Y., Peng, L., and Lin, J. (2015). Monitoring the performance of the building attached photovoltaic (BAPV) system in Shanghai. *Energy and Buildings*, Vol. 88, pp. 174–182. DOI: 10.1016/j.enbuild.2014.11.073.

Xiang, C. and Matusiak, B. S. (2022). Façade Integrated Photovoltaics design for high-rise buildings with balconies, balancing daylight, aesthetic and energy productivity performance. *Journal of Building Engineering*, Vol. 57, 104950. DOI: 10.1016/j.jobe.2022.104950.

Xiong, W., Liu, Z., Wu, Z., Wu, J., Su, F., and Zhang, L. (2022). Investigation of the effect of Inter-Building Effect on the performance of semi-transparent PV glazing system. *Energy*, Vol. 245, 123160. DOI: 10.1016/j.energy.2022.123160.

Xuan, Q., Li, G., Lu, Y., Zhao, B., Wang, F., and Pei, G. (2021). Daylighting utilization and uniformity comparison for a concentrator-photovoltaic window in energy saving application on the building. *Energy*, Vol. 214, 118932. DOI: 10.1016/j.energy.2020.118932.

Zomer, C. and Rüther, R. (2017). Simplified method for shading-loss analysis in BIPV systems. Part 2: Application in case studies. *Energy and Buildings*, Vol. 141, pp. 83–95. DOI: 10.1016/j.enbuild.2017.02.043.

ОПТИМИЗАЦИЯ КОНФИГУРАЦИИ ИНТЕГРИРОВАННЫХ В ЗДАНИЕ ПРОЗРАЧНЫХ ФОТОЭЛЕКТРИЧЕСКИХ СИСТЕМ С УЧЕТОМ ДНЕВНОГО СВЕТА И ЭНЕРГОЭФФЕКТИВНОСТИ В ШКОЛЬНЫХ ЗДАНИЯХ В ТРОПИКАХ

Сьюзан Сьюзан[1,2]*, Сафиал Акбар бин Закария[1], Шарифа Файруз Сайед Мохд Фадзил[1]

[1] Университет Сайнс Малайзия, Пенанг, Малайзия
[2] Университет Чипутра Сурабая, Сурабая, Восточная Ява, Индонезия

*E-mail: susan@student.usm.my / susan@ciputra.ac.id

Аннотация
Введение: Использование вертикальных фасадов для бокового освещения рассматривается в многочисленных исследованиях. Установлено, что вертикальные фасады представляют собой эффективное средство обеспечения доступа дневного света, которое помогает создать приятную атмосферу, повысить успеваемость в школах и улучшить здоровье обучающихся. Недавние исследования также выявили потенциал использования вертикальных фасадов в высотных зданиях в качестве интегрированных в здание фотоэлектрических систем (BIPV) благодаря большой доступной площади. В тропиках такое потенциальное применение также обусловлено большим количеством солнечного света. Технология прозрачных фотоэлектрических систем (TPV) дает возможность удовлетворить обе потребности. В зависимости от ряда факторов, таких как коэффициент пропускания видимого света (VT) и количество ячеек, она обеспечивает боковое освещение и применяется в интегрированных в здание прозрачных фотоэлектрических системах (BITPV). Для бокового освещения требуется более высокий коэффициент пропускания видимого света (VT), который позволит обеспечить оптимальное проникновение дневного света. При этом для интегрированных в здание прозрачных фотоэлектрических систем (BITPV) предпочтительно большее количество ячеек и более низкий коэффициент пропускания видимого света (VT). Предыдущие исследования показали, что интегрированные в здание прозрачные фотоэлектрические системы (BITPV) предлагаются для зданий с соотношением площади окна к площади стены (WWR) в 45 % и более, которое кажется довольно высоким для зданий, располагающихся в тропиках, где соотношение WWR обычно предлагается в диапазоне 30–40 %. **Цель исследования:** Данное исследование направлено на поиск оптимальной конфигурации и представление систематического метода оптимизации интегрированных в здание прозрачных фотоэлектрических систем (BITPV) фасадов школ в тропиках. **Методы:** Для достижения поставленной цели использован экспериментальный подход с применением моделирования. В качестве объекта исследования был выбран участок с планировкой, типичной для школ, располагающихся в тропиках. Для формирования пост-экспериментальных моделей был учтен коэффициент пропускания видимого света (VT) и количество ячеек. **Результаты и обсуждение:** В тропиках при использовании фотоэлектрических систем с низкой прозрачностью, интегрированные в здание прозрачные фотоэлектрические системы (BITPV) с соотношением площади окна к площади стены (WWR) 31,25 % и 30 % коэффициентом покрытия ячейками обеспечивают оптимальный визуальный комфорт и энергоэффективность. При этом интегрированные в здание прозрачные фотоэлектрические системы (BITPV) с соотношением площади окна к площади стены (WWR) 31,25 % и 50 % коэффициентом покрытия ячейками представляют собой оптимальную конфигурацию при использовании фотоэлектрических систем с высокой прозрачностью. В данном исследовании также представлен систематический метод проектирования интегрированных в здание прозрачных фотоэлектрических систем (BITPV) для многоэтажных школьных зданий в тропиках.

Ключевые слова: интегрированные в здание прозрачные фотоэлектрические системы (BITPV), энергозамещение, освещенность, школьное здание, тропики.